Chemistry & Biology, Vol. 9, 1129–1139, October, 2002, ©2002 Elsevier Science Ltd. All rights reserved. PII S1074-5521(02)00242-9

Rational Structure-Based Design of a Novel Carboxypeptidase R Inhibitor

Eliada Lazoura,[1] William Campbell,[2] Yoshiki Yamaguchi,[3] Koichi Kato,[3] Noriko Okada,[1] and Hidechika Okada[1,4]

[1]Department of Molecular Biology
School of Medicine
Nagoya City University
Mizuho-ku, Nagoya 467-8601
Japan

[2]Choju Medical Institute
Fukushimura Hospital
Toyohashi 441-8124
Japan

[3]Department of Structural Biology and Biomolecular Engineering
Graduate School of Pharmaceutical Sciences
Nagoya City University
Mizuho-ku, Nagoya 467-8603
Japan

Summary

A novel carboxypeptidase R (CPR) inhibitor, related to potato carboxypeptidase inhibitor (PCI), was designed using rational structure-based strategies, incorporating two principle facts: CPR has a strong affinity for basic amino acids, and the two lysine and arginine residues of PCI are orientated in the same direction and held in close spatial proximity by three disulfide bonds. Initially, a disulfide-bonded fragment of PCI was synthesized showing weak competitive inhibitory activity against CPR. Subsequently, a smaller linear 9-mer peptide, designated CPI-2KR, was designed/synthesized and found to be a more efficient competitive inhibitor of CPR, without affecting the activity of the other plasma carboxypeptidase, carboxypeptidase N. In vitro studies showed that, together with tissue plasminogen activator, CPI-2KR synergistically accelerated fibrinolysis, representing a lead compound for the design of smaller organic molecules for use in thrombolytic therapy.

Introduction

Carboxypeptidases (CPs) are enzymes that catalyze the hydrolysis of peptide bonds at the C termini of peptides and proteins. Briefly, they have been categorized according to two principle mechanisms of action: as metallocarboxypeptidases (MPs) or cysteine/serine-carboxypeptidases (Cys/Ser-CP). MPs are distinct from Cys/Ser-CPs in that they possess a tightly bound Zn^{2+} atom, which is directly involved in catalysis, while Cys/Ser-CPs contain a reactive Cys/Ser residue at the active site similar to the Ser/His/Asp triad of serine proteases. MPs can be further subdivided into carboxypeptidase A-like enzymes, which have a preference for hydrophobic C-terminal residues, and carboxypeptidase B-like enzymes, which have a preference for C-terminal basic residues (lysine and arginine). For review, see Vendrell et al. [1].

Carboxypeptidase R (CPR) [2]–also known as plasma carboxypeptidase B (CPB) [3], carboxypeptidase U (CPU) [4], or activated thrombin-activatable fibrinolysis inhibitor (TAFIa) [5]–is a carboxypeptidase B-like enzyme present as a zymogen (proCPR) in plasma. CPR plays a crucial role in the regulation of fibrinolysis [3, 6] and acts as an inactivator of inflammatory mediators, preferentially removing C-terminal arginine (R) residues from anaphylatoxins, thereby preventing excess inflammation [7]. Carboxypeptidase N (CPN; 270 kDa glycoprotein) [8], which is also present in plasma, is also an important inactivator of anaphylatoxins, kinins, and fibrinopeptides [9–11]. However, in contrast to CPR, it does not play any significant role in dampening fibrinolysis. Moreover, CPN is present in the active form in plasma, whereas CPR is found in the inactive proCPR state and is called into play during coagulation [2]. Previously, the carboxypeptidase activity in plasma responsible for inactivation of bradykinin, anaphylatoxins, and other basic carboxy-terminal peptides was considered to be due only to CPN [9–11]. However, CPR was also shown to inactivate bradykinin and anaphylatoxin octapeptides [12, 13]; furthermore, CPR, but not CPN, was found to effectively reduce fibrinolysis [14].

As shown in Figure 1, following activation, CPR catalyses the removal of C-terminal lysine (K) residues from cell-surface proteins and partially degraded fibrin clots, thereby preventing the binding [15, 16] and activation of plasminogen [5, 14]. Conversion of plasminogen (Glu-plasminogen) to its active form, plasmin (Lys-plasmin or Lys-plasminogen), requires tissue-plasminogen activator (t-PA), which is an activator of blood clot lysis. Binding of t-PA to fibrin, via its K binding domain, catalyses cleavage of Glu-plasminogen (i.e. plasminogen) at the C terminus of Lys76 to yield Lys-plasminogen (i.e. plasmin). Lys-plasminogen has an increased affinity for fibrin compared to Glu-plasminogen, since the release of residues 1–76 exposes the kringle 1 domain, which contains two residues (Arg32 and Arg34), previously shown to be responsible for fibrin binding [17]. Studies have shown that CPR inhibits t-PA-induced lysis only when Glu-plasminogen, but not Lys-plasminogen, is present, suggesting that its antifibrinolytic effect is primarily mediated through inhibition of Glu-plasminogen activation [5]. Therefore, removal of Lys-residues by CPR from partially degraded fibrin diminishes the already low binding affinity of Glu-plasminogen to fibrin, essentially prolonging fibrinolysis [3]. Plasmin-mediated proteolysis of fibrin constitutes a positive-feedback process that enhances plasminogen activation. CPR inhibits fibrinolysis by removing C-terminal lysine residues from fibrin, thereby limiting plasmin formation [5, 13, 14].

At present, t-PA is the only treatment for thromboembolic stroke approved by the Food and Drug Administration. However, adverse side effects have recently been

[4]Correspondence: hiokada@med.nagoya-cu.ac.jp

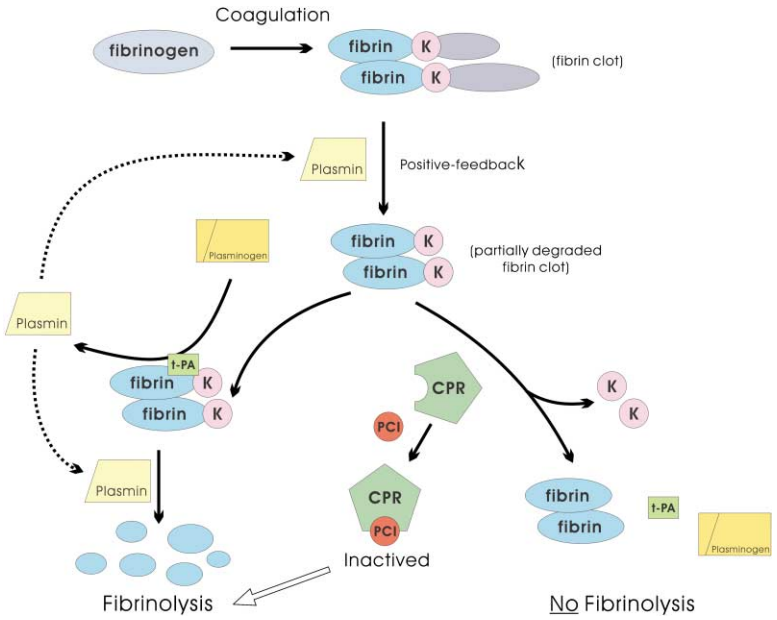

Figure 1. Coagulation and Fibrinolysis Pathway

The action of CPR on fibrinolysis in the presence/absence of PCI is shown.

reported in some patients, suggesting that t-PA may modulate *N*-methyl-D-aspartate (NMDA)-receptor-mediated signaling and excitotoxic neuronal death [18]. To alleviate this problem, the coadministration of potato carboxypeptidase inhibitor (PCI) with lower doses of t-PA has been suggested, and recent experiments in animal models have shown that PCI dramatically enhances clot lysis [19]. PCI [20] is a small 39-residue protein (MW 4295 Da) that has the ability to selectively inhibit CPR (Figure 1) without affecting the activity of CPN in the circulation [14]. An understanding of the interaction between CPR and PCI is crucial for the development of novel therapeutics for use in thrombolytic therapy. Our studies have lead to the design of a smaller peptide inhibitor of CPR, designated CPI-2KR, which shows similar biological activity to PCI in vitro and is a competitive inhibitor of CPR. While this peptide may be useful for the treatment and/or prevention of thrombosis, it also represents a starting point for the design of low molecular weight organic molecules, which are preferable and more useful alternatives. In this report, the rational structure-based strategies employed to design the novel CPR inhibitor are discussed.

Results and Discussion

Requirement of CPR Inhibitor

The mechanisms involved in the regulation of coagulation and fibrinolysis (clot lysis) are complex and include numerous protein-protein interactions. Of particular interest has been the recent discovery of proCPR (58 kDa glycoprotein), a metallocarboxypeptidase found in the plasma exhibiting carboxypeptidase B-like activity following activation. Proteolytic cleavage at Arg92 yields a 92 amino acid activation peptide ($\sim$15 kDa) and a 309 amino acid enzyme (CPR; 35 kDa). The inactive proCPR form is present in the plasma at concentrations between 70 and 275 nM, 50-fold lower than the K_m value for activation [21]. Although proCPR can be activated by thrombin, the process is inefficient (K_m 0.5–2.1 μM; k_{cat} 0.0021 s^{-1}), requiring large amounts of thrombin compared to activation by plasmin (K_m 55 nM; k_{cat} 0.00044 s^{-1}) [22]. In contrast, the complex formed between thrombin and the endothelial cell receptor, thrombomodulin (TM), can more efficiently activate this zymogen (k_{cat} 0.4–1.2 s^{-1}) [22, 23]. Since proCPR is activated by thrombin, enzymes that regulate the formation of thrombin, such as protein C, are also most likely involved. Furthermore, the activation of both protein C and proCPR is enhanced when thrombin is bound to TM, which is subsequently liberated into the plasma [22, 24]. Recent studies have showed that although higher TM concentrations (10 and 25 nM) upregulated fibrinolysis, attributed to the activation of protein C, lower TM concentrations ($<$5 nM) resulted in downregulation of fibrinolysis due to proCPR activation [25].

Recently, proCPR has been shown to be an acute phase protein, with upregulation of its mRNA in response to inflammation [26, 27]. On the other hand, in diseases where circulating TM levels are elevated, such as diabetes mellitus with microangiopathy, disseminated intravascular coagulation (DIC), and systemic lupus erythromatosus, its upregulation may result in enhanced susceptibility to thrombosis. It has been shown that proCPR levels exceeding 129 nM correlate with a 2-fold increase in risk for deep vein thrombosis [28]. Therefore, the development of a CPR inhibitor for use in thrombolytic therapy is highly desirable.

Inhibitor Design Concept

To date, no physiological inhibitor of CPR has been isolated, although metallocarboxypeptidase inhibitors have been found in potatoes [20], tomatoes [29], roundworms [30], leeches [31], and some mammalian tissues [32]. Of these, potato carboxypeptidase inhibitor (PCI; $K_i = 0.4$ nM) is the most extensively studied. Additionally, the nonspecific sulfur-containing analog of arginine, guanidinoethylmercaptosuccinic acid (GEMSA; K_i = 18

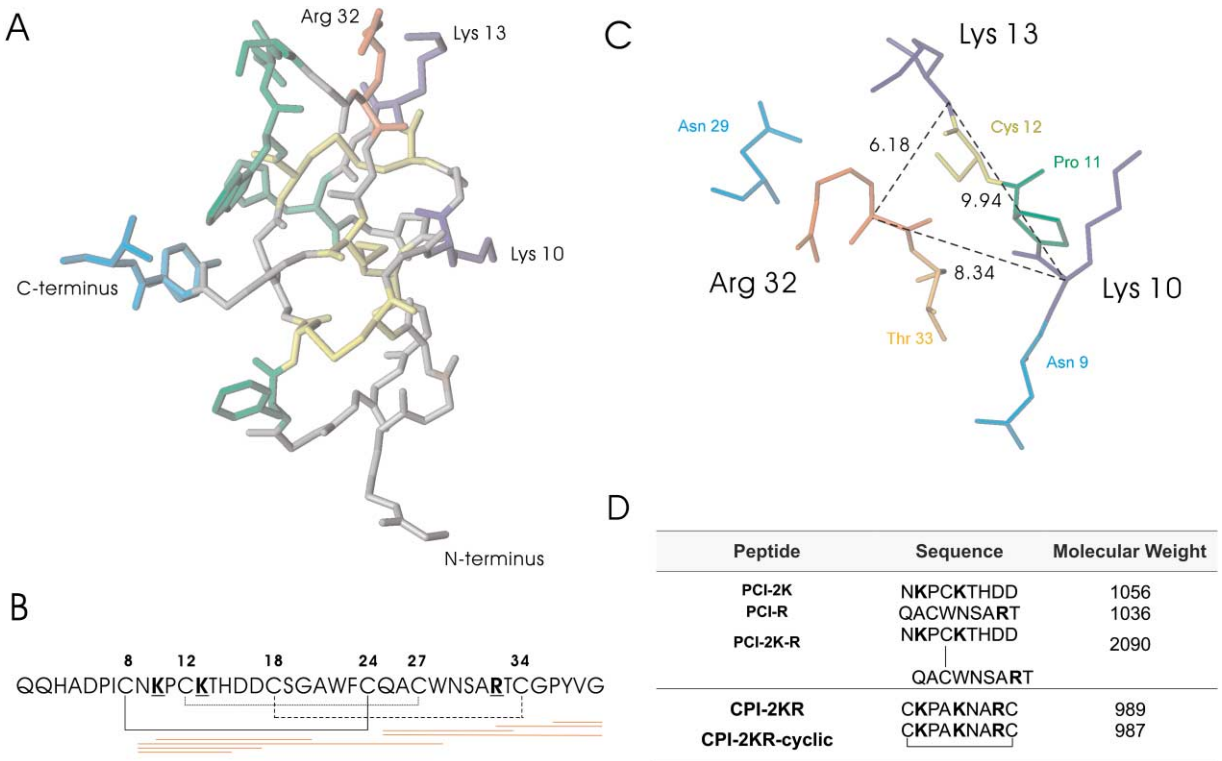

Peptide	Sequence	Molecular Weight
PCI-2K	NKPCKTHDD	1056
PCI-R	QACWNSART	1036
PCI-2K-R	NKPCKTHDD | QACWNSART	2090
CPI-2KR	CKPAKNARC	989
CPI-2KR-cyclic	CKPAKNARC	987

Figure 2. Potato Carboxypeptidase Inhibitor (PCI)

(A) Crystal structure of PCI from 4CPA showing the primary (cyan) and secondary (green) binding sites of PCI to CPA. In addition, the two lysine (blue) and single arginine (red) residues we believe to be responsible for inhibiting CPR are highlighted. Disulfide bridges are shown in yellow.

(B) Sequence of PCI showing the disulfide bond configuration (Cys8–Cys24, Cys12–Cys27, and Cys18–Cys34). The basic residues are shown in bold and underlined. The PCI-derived peptide fragments synthesized and assayed for inhibitory activity against CPR are underlined in red.

(C) Partial crystal structure of PCI, showing the spatial arrangement of the basic residues (Lys10, Lys13, and Arg32). The C_α-C_α distances (indicated by the dotted lines; Å) between Lys10, Lys13, and Arg32 are shown.

(D) Sequences and molecular weight of the PCI-derived peptides (PCI-2K, PCI-R, and PCI-2K-R), our novel inhibitory peptide (CPI-2KR), and CPI-2KR-cyclic.

μM), inhibits CPR [33]. However, although GEMSA is a potent CP inhibitor, it cannot differentiate between CPR and CPN, precluding its use for therapeutic applications. Nonetheless, the physicochemical properties of this small organic molecule were incorporated into the design of our novel CPR inhibitor.

Due to its ability to inhibit CPR but not CPN, PCI has frequently been used to assess CPR activity both in vitro [22, 34] and in vivo [19, 35]. Supplementing t-PA doses with PCI has been shown to enhance thrombolytic therapy in an animal model [19]. However, it should be noted that although PCI selectively inhibits CPR in the circulation, it also inhibits CPs found in the digestive tract (pancreatic CPB), brain, pituitary, pancreatic islet, and other neuroendocrine cells (CPE/CPH), possibly causing other serious side effects upon administration [36]. Therefore, the development of a more specific CPR inhibitor of low molecular weight without toxicity is highly desirable.

PCI is a 39 amino acid protein belonging to the cystine knot family [37]. Due to the presence of three disulfide bonds (Figure 2A), it has a compact structure, comprising a globular core (Cys8–Cys34) and flexible N and C termini (Glu1–Ile7 and Glu35–Lys39, respectively). At present, no structural data is available for CPR due to its instability; however, the structure of PCI complexed with carboxypeptidase A (CPA) is available, which shows that PCI binds to CPA through its C terminus [38, 39]. Although the specificity of CPA and CPR differs, the current assumption is that PCI also binds to CPR through its C terminus. Our studies, however, have shown that the tetrapeptide C-terminal fragment of PCI could neither reverse the TM-induced retardation of t-PA-induced fibrinolysis (in vitro fibrinolysis assay) nor decrease CPR activity to inhibit hippuryl-L-arginine cleavage (data not shown). In addition, other longer N- and C-terminal peptide fragments of PCI (Figure 2B) also showed no inhibitory activity against CPR (data not shown), suggesting that the mechanism of inhibition is more complex.

Studies on leech carboxypeptidase inhibitor (LCI) have revealed nonspecific removal of the C-terminal Glu66 residue by both pancreatic CPA2 and CPB, which have a restricted specificity for aromatic and positively charged C-terminal residues, respectively. Although the removal mechanism remains a mystery, no decrease in inhibitory activity was observed [31]. Similarly, X-ray crystallographic analysis of PCI complexed to CPA re-

A

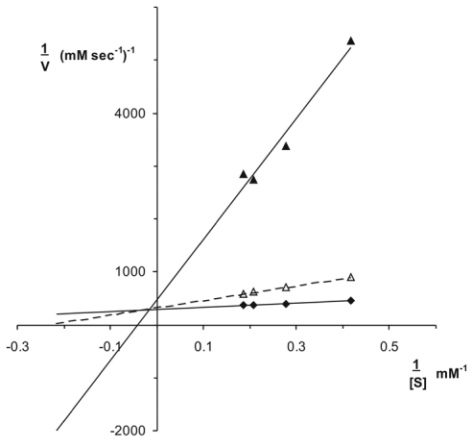

B

Inhibitor (I)	[I] (nM)	K_m (mM)	V_{max} (mM·sec^{-1})	k_{cat} (sec^{-1})	K_i (nM)	R^2
None	0	1.27	0.0034	0.0027	N/A	0.992
PCI	12	12.3	0.0012	0.0001	1.4	0.964
PCI-2K-R	239	4.2	0.0021	0.0008	407.1	0.998

[CPR] = 8.8 mmol/L

C

QQHADPICN**K**
QHADPICN**K**P
HADPICN**K**PC
ADPICN**K**PC**K**
DPICN**K**PC**K**T
PICN**K**PC**K**TH
ICN**K**PC**K**THD
CN**K**PC**K**THDD
N**K**PC**K**THDDC
KPC**K**THDDCS
PC**K**THDDCSG
C**K**THDDCSGA
KTHDDCSGAW
THDDCSGAWF
HDDCSGAWFC
DDCSGAWFCQ
DCSGAWFCQA
CSGAWFCQAC
SGAWFCQACW
GAWFCQACWN
AWFCQACWNS
WFCQACWNSA
FCQACWNSA**R**
CQACWNSA**R**T
QACWNSA**R**TC
ACWNSA**R**TCG
CWNSA**R**TCGP
WNSA**R**TCGPY
NSA**R**TCGPYV
SA**R**TCGPYVG

Figure 3. Competitive Inhibition of PCI and PCI-2K-R against CPR

(A) Lineweaver-Burke plot plot (1/v versus 1/[S]) for PCI (closed triangle) and PCI-2K-R (open triangle) showing competitive inhibition relative to no inhibitor (closed diamond).

(B) Kinetic constants (V_{max}, K_m, k_{cat}, and K_i) for CPR alone and in the presence of PCI and PCI-2K-R. The R^2 values for the linear regressions are included.

(C) CPR binding to PCI-derived 10-mer peptides on a cellulose membrane. The thick bold line indicated the peptides that bound CPR. Basic residues are shown in bold.

vealed that the C-terminal Gly39 residue was also removed [38, 39]. Likewise, the removal mechanism of the nonspecific C-terminal Gly39 residue of PCI by CPA is unclear, however, it has been proposed to facilitate coordination of the newly generated C-terminal Val38 residue of PCI to the catalytic active site of CPA [31].

In contrast to these studies, our results suggest that the C terminus of PCI may not be responsible for its inhibitory activity against CPR. Since the function of CPR is to remove C-terminal Lys and Arg residues from fibrin clots and inflammatory mediators, respectively, we investigated the possibility that PCI inhibits CPR by competitively binding via these residues of PCI. Close inspection of the X-ray structure of PCI complexed to CPA [38, 39] revealed that the two Lys residues and a single Arg residue of the former are orientated in the same direction (Figure 2A). Furthermore, although these residues are far from each other in the linear sequence of PCI, the disulfide bonding configuration brings them in close proximity to one another (Figure 2C), directly opposite the primary (residues 37–39) and secondary (residues 15, 23, 28, 29, and 30) binding domains of PCI for CPA (Figure 2A). The possible involvement of these basic residues for the inhibition of CPR was subsequently examined.

Heterodimeric Peptide

We designed and synthesized two peptide fragments which mimicked the PCI regions possibly responsible for the observed inhibitory activity. The first peptide (PCI-2K) contained the two lysine residues and the second peptide (PCI-R) contained the arginine residue (Figure 2D). These peptides represent two regions of PCI maintained in close spatial proximity by three disulfide bridges. As a starting point, under high dilution conditions, equimolar amounts of peptides PCI-2K and PCI-R, both containing a single cysteine residue, were oxidized to form the heterodimer PCI-2K-R. In contrast to the monomeric peptides, for which no activity was observed (data not shown), the heterodimer, PCI-2K-R, was found to be a weak competitive inhibitor of CPR (Figure 3A). Furthermore, kinetics studies revealed that compared to PCI (K_m 12.3 μM; K_i 1.4 nM; Figure 3B), the inhibitory activity of PCI-2K-R was 290-fold lower (K_m 4.2 μM; K_i 407.1 nM; Figure 3B). The reduced inhibitory activity of this PCI-derived peptide may be attributed to the absence of two of the three disulfide bridges found in wild-type PCI, effectively resulting in increased mobility of all residues. To support these results, the interaction between CPR and 10-mer PCI peptide fragments synthesized on a cellulose membrane was also examined. The results, shown in Figure 3C, indicated that CPR bound with peptides containing two Lys residues and also with peptides containing an Arg residue at their N terminus. Inaccessible Lys and Arg residues, located proximal to the membrane, did not interact appreciably with CPR. It should be noted that while the cellulose binding experiments provide relevant information on

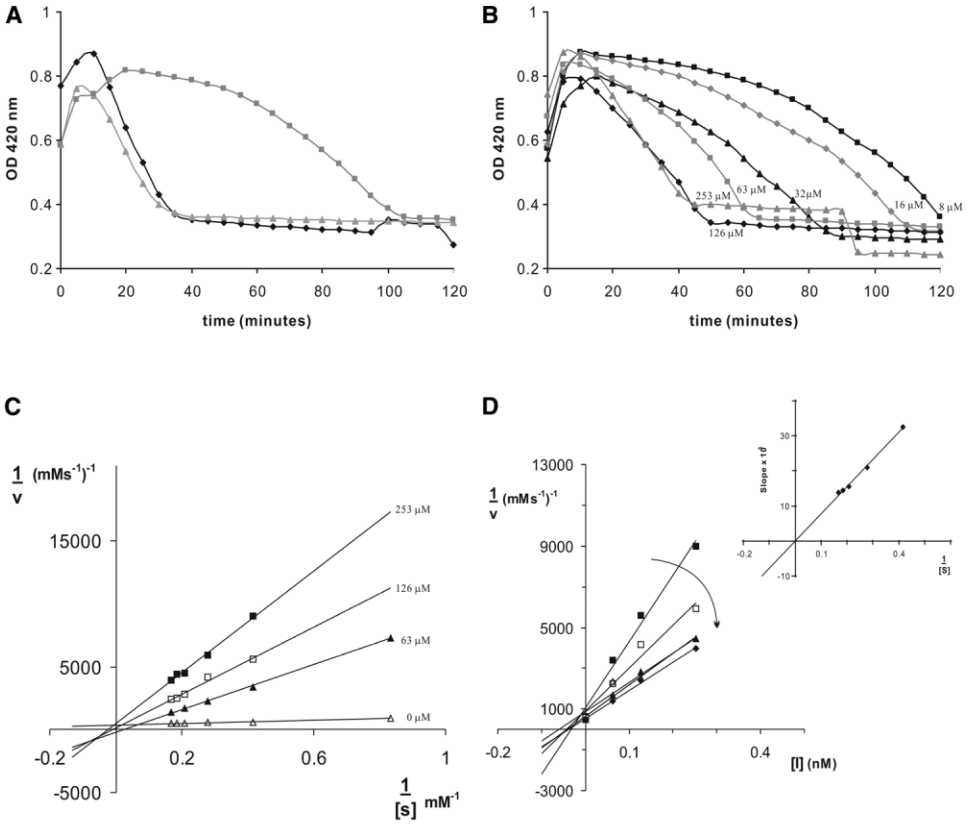

E

Inhibitor (I)	[I] (nM)	K_m (mM)	V_{max} (mM·sec^{-1})	k_{cat} (sec^{-1})	K_i (nM)	R^2
None	0	1.4	0.0025	0.001081	N/A	0.991
CPI-2KR	253	41.7	0.0021	0.000049	8.8	0.991

[CPR] = 1.1 mmol/L

Figure 4. Competitive Inhibition of CPI-2KR against CPR

(A) In vitro TM-induced retardation (gray squares) of t-PA-induced fibrinolysis (gray triangles) due to the conversion of proCPR to CPR by the T/TM complex. Inhibition of CPR by PCI (12 μM) is indicated by reversal of the TM-induced retardation of t-PA-induced fibrinolysis (black diamonds).

(B) Dose-dependent inhibition by CPI-2KR at various concentrations (8, 16, 32, 63, 126, and 253 μM) on the TM-induced retardation of t-PA-induced fibrinolysis.

(C) Lineweaver-Burke plot (1/v versus 1/[S]) for CPI-2KR at various concentrations (63, 126, and 253 nM) relative to no inhibitor (0 μM).

(D) Dixon Plot (1/v versus [I]) for CPI-2KR for increasing substrate concentrations (1.2–6.0 mM; indicated by arrow). Replotting of slopes of Dixon plot versus 1/[S] showing competitive inhibition (inset).

(E) Kinetic constants (V_{max}, K_m, k_{cat}, and K_i) for CPR alone and in the presence of CPI-2KR. The R^2 values for the linear regressions are included.

possible PCI binding domains, they do not provide corresponding information on the actual biological activity. Furthermore, the observed interaction may be influenced/enhanced by polyvalency effects.

In human plasma, t-PA-induced fibrinolysis is suppressed by the addition of TM (<10 nM). This suppression could be due to the conversion of proCPR to its active CPR form, which is inhibited by the presence of PCI (12 nM), thus permitting fibrinolysis to proceed (Figure 4A). However, the heterodimeric peptide PCI-2K-R could not reverse the TM-induced retardation of t-PA-induced fibrinolysis (data not shown). The competitive inhibition of PCI-2K-R might not be strong enough to support t-PA function.

Novel Linear Peptide Inhibitor

In view of the promising results obtained for the peptide PCI-2K-R, the crystal structure of PCI was more closely examined. In particular, the spatial C_α-C_α distances between the Lys and Arg residues were measured (Figure

A

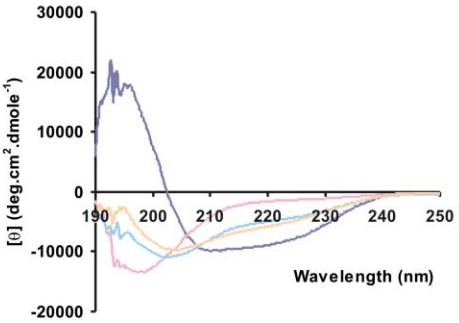

B

	α-Helix	β-Sheet	β-Turn	Random
CPR	35.9	38.1	11.0	15.0
CPI-2KR	0.0	16.2	19.6	64.2
Complex$_0$	3.0	48.3	8.6	40.1
Complex$_{30}$	4.9	50.8	7.9	36.4

Figure 5. CD Spectra of CPR, CPI-2KR, and the CPR/CPI-2KR Complex

(A) CD spectra of CPR (dark blue), CPI-2KR (pink), and the CPR/CPI-2KR complex immediately after mixing (Complex$_0$; light blue) and 30 min after mixing (Complex$_{30}$; gold). Spectra were recorded at 4°C in Tris-HCl (50 mM, pH 7.5).

(B) Secondary structure estimations determined for the CD spectra shown in (A).

2C). Subsequently, a novel linear peptide (CPI-2KR, CKPAKNARC; Figure 2D) was designed based on the data obtained from PCI. The peptide included the two Lys and one Arg residues from PCI (Lys10, Lys13, and Lys32) expected to be responsible for the interaction observed between PCI and CPR. The spatial separation of these basic residues was approximated to resemble that of PCI. In addition, the proline (Pro11) residue adjacent to the Lys10 residue and the alanine (Ala31) residue adjacent to the Arg32 residue of PCI were included. At the N and C termini, cysteine (Cys) residues were added so as to permit cyclization of the peptide and reduce conformational flexibility (CPI-2KR-cyclic; Figure 2C). The Cys residue between the two Lys residues (Lys10 and Lys13; Figure 2C) was replaced by an Ala residue to remove any possible interference with cyclization.

Peptide CPI-2KR was assayed for its ability to reverse the TM-induced retardation of t-PA-induced fibrinolysis. Remarkably, this short linear peptide showed dose-responsive inhibition of TM-induced retardation of t-PA-induced fibrinolysis (Figure 4B), although the effective inhibitory concentration of CPI-2KR (126 nM) was 10-fold lower that of PCI (12 nM). In contrast, cyclization of the peptide (CPI-2KR-cyclic) resulted in a dramatic loss of inhibitory activity (data not shown), indicating that a certain degree of structural mobility may be necessary for the peptide to adopt the correct conformation for binding to CPR. Furthermore, mutation studies indicated that the basic and Cys residues of CPI-2KR are essential for inhibitory activity. In particular, replacement of the basic residues by alanine residues, removal of the N- and C-terminal Cys residues, or replacement of these residues by either Ala or methionine (Met) resulted in a loss of biological activity (data not shown).

Mechanism of Inhibition

In order to gain insight into the inhibitory mechanism of CPI-2KR against CPR, a classical Henri-Michaelis-Menten kinetics analysis was performed. Since the Lineweaver-Burke plot (Figure 4C) is prone to error, particularly at low concentrations of inhibitor and substrate, the Dixon plot (1/v *versus* [I]) was employed to evaluate the inhibitory mechanism of CPI-2KR (Figure 4D). Replotting of the slopes of the Dixon plot against 1/[S] confirmed that CPR-2KR is a competitive inhibitor of CPR, given that the line went through the origin (Figure 4D, inset). The K_m, $K_{m_{app}}$, *and* V_{max} were determined from the data obtained for no inhibitor and the highest inhibitor concentration (253 nM) from the Lineweaver-Burke plots (Figure 4E). These values were in turn used to calculate the dissociation constant of CPI-2KR (K_i). CPI-2KR was found to have a relatively low K_i (8.8 nM; 6-fold higher than that of PCI), indicating that it binds to CPR with a relatively strong affinity. Of particular interest is the significant improvement in binding affinity for CPR (~46-fold stronger than PCI-2K-R), with the observed concomitant increase in inhibitory activity, when compared to PCI-2K-R. This may be attributed to the close spatial proximity of the K and R residues in the absence of disulfide bridges, as for PCI.

Structure Studies

Using similar conditions to those of the enzyme kinetics studies, circular dichroism (CD) spectroscopy was employed to analyze the solution conformation of CPR alone and when complexed with CPI-2KR. Due to the instability of CPR, the studies were performed at 4°C. After mixing CPI-2KR (150 μM) with CPR (1.1 μM), a significant change in the CD spectrum was observed (Figure 5A). The peptide is predominantly in a random conformation, and CPR predominantly displays α-helical and β sheet structure (Figure 5B). The CD spectra of the CPR/CPI-2KR complex immediately after mixing (Complex$_0$) shows a significantly less random structure, particularly after 30 min incubation at 4°C (Complex$_{30}$), suggesting that the conformation of CPR was altered when the CPR/CPI-2KR complex was formed. PCI, which predominantly contains β sheet structure, was also complexed with CPR as a control. Similarly, a conformational change was observed when the CPR/PCI was formed. In particular, a slight increase in α-helical structure was observed with a concomitant increase in random structure and decrease in β sheet structure (data not shown).

A

Peptide	C_α-C_α distance (Å)		
	Lys2 – Lys5	Lys5 – Arg8	Arg8 – Lys2
PCI-2K-R	6.23	10.55	9.74
CPI-2KR	9.03	7.32	4.27
CPI-2KR-cyclic	7.19 (8.02)[a]	10.20 (6.89)[a]	6.20 (6.19)[a]
PCI	9.94[b]	6.18[b]	8.34[b]

[a] NMR-derived structure values in brackets (RMSD between model and NMR structure is 3.1 Å).
[b] Lys10 – Lys13, Lys13 – Arg32 and Arg32 – Lys10 distances.

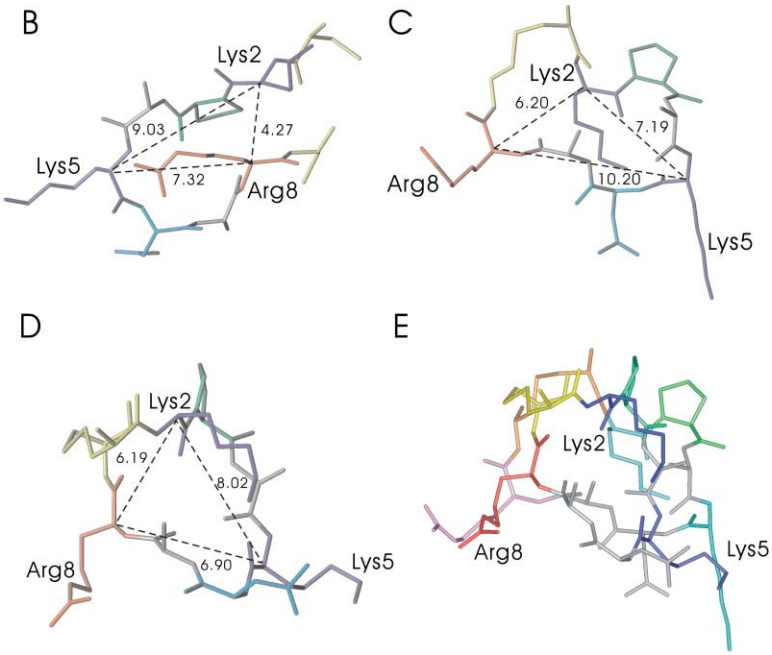

Figure 6. NMR and Molecular Modeling Studies

(A) C_α-C_α distance (Å) between the basic residues of PCI-2K-R, CPI-2KR, CPI-2KR-cyclic, and PCI.

(B) Energy minimized structure of CPI-2KR showing the C_α-C_α distance (Å) between the basic residues.

(C) Energy minimized structure of CPI-2KR-cyclic showing the C_α-C_α distance (Å) between the basic residues.

(D) NMR structure of CPI-2KR-cyclic showing the C_α-C_α distance (Å) between the basic residues.

(E) NMR structure of CPI-2KR-cyclic (Arg in red, Lys in blue, Cys in yellow, and Pro in green) superimposed on energy minimized structure (Arg in pink, Lys in cyan, Cys in orange, and Pro in mint).

Nuclear magnetic resonance (NMR) and molecular modeling (MM) studies provided insight into the possible conformation of the cyclic and linear peptides. Preliminary MM studies revealed that CPI-2KR can adopt a conformation with Lys and Arg residue C_α-C_α distances comparable to those of PCI (Figure 6A). The lowest energy conformation, following high-temperature simulated annealing energy minimization, is shown in Figure 6B. Although the Arg8–Lys2 C_α-C_α distance is almost half that of PCI, this peptide is flexible enough, due to the lack of a disulfide bridge between the terminal Cys residues, to adopt a more suitable conformation to bind

A

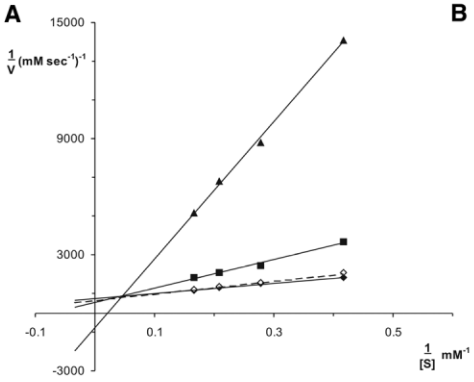

B

Inhibitor (I)	[I] (nM)	K_m (mM)	V_{max} (mM·sec^{-1})	k_{cat} (sec^{-1})	R^2
None	0	3.47	0.0013	0.00039	0.990
GEMSA	425	14.1	0.0019	0.00014	0.994
GEMSA	2126	N/A*	N/A*	0.00003	0.985
CPI-2KR	506	5.16	0.0015	0.00030	0.997

* N/A, not applicable

Figure 7. Inhibition of CPN by GEMSA But Not by CPI-2KR

(A) Lineweaver-Burke plot (1/v versus 1/[S]) for GEMSA (closed square and closed triangle; 425 and 2126 nM, respectively) and CPI-2KR (open diamonds; 506 nM) relative to no inhibitor (closed diamond).

(B) Kinetic constants (V_{max}, K_m, and k_{cat}) for CPN alone and in the presence of GEMSA and CPI-2KR. The R^2 values for the linear regressions are included.

to CPR. For comparison, the cyclic peptide (CPI-2KR-cyclic) was also subjected to this procedure (Figure 6C); however, due to steric hindrance, the C_α-C_α distances of Lys and Arg were significantly different from those of PCI (Figure 6A). Although NMR spectroscopy could not provide any structural information for the linear peptide due to the large conformational flexibility of the molecule, the cyclic peptide structure was deduced (Figure 6D). From this data, we can see that the spatial separation of the Lys and Arg residues, for both the model and NMR structures of CPI-2KR-cyclic, significantly differs from that of PCI. Furthermore, the C_α-C_α distances of Lys and Arg of the NMR structure of CPI-2KR-cyclic significantly differed from those of model structure obtained using the high-temperature simulated annealing protocol. However, despite this, our studies showed that a cyclic 9-mer peptide cannot have all basic residue side chains facing in the same direction (Figure 6E). In both cases, one of the Lys residues is in the down position, while the other Lys and the Arg residues are in the up position. Therefore, CPI-2KR-cyclic might be unable to adopt a suitable conformation for binding to CPR due to steric hindrance.

No Effect on Carboxpeptidase N

Finally, as shown in Figure 7, CPI-2KR did not exhibit any inhibitory activity against CPN even at 506 nM, 2-fold higher than the concentration required for CPR inhibition (Figure 7). In contrast, GEMSA, which inhibits CPR at 18 μM [40], inhibited CPN at a lower concentration of 425 nM.

Significance

CPI-2KR was designed using a rational structure-based strategy which combined information obtained from the crystal structure of a known CPR inhibitor, namely PCI, and the biological known function of the enzyme. Taken together, the information yielded a successful peptide candidate, which effectively lowered the TM-induced retardation of t-PA-induced fibrinolysis similar to PCI, acting through a competitive inhibitory mechanism, specifically inhibiting CPR without affecting CPN. This small novel CPR inhibitor is thus a useful agent for use in the prevention and/or treatment of thrombosis, while representing a lead molecule for the design of smaller organic molecules for use as adjuncts to thrombolytic therapy.

Experimental Procedures

Peptide Synthesis

Peptides were synthesized using an AMS 422 Multiple Peptide Synthesiser (ABiMED, Langenfeld, Germany) using standard solid-phase synthesis techniques and 9-fluorenylmethoxycarbonyl (Fmoc) amino acids (Watanabe Chemical Industries Ltd., Hiroshima, Japan). In situ activation was by 2-(1H-Benzotriazole-1-yl)-1,1,3,3-tetramethyluronium hexafluorophosphate (HBTU) with *N*-methylmorpholine (NMM) and hydroxybenzotriazole (HOBT) as catalytic bases. Amidated peptides (25 μmole scale) were prepared using Fmoc-PAL-PEG-PS resin (PerSeptive Biosystems; Warrington, UK). All residues were double coupled in *N*,*N*-dimethylformamide (DMF; Peptide synthesizer grade; Watanabe Chem. Ind. Ltd.) *N*-methylpyrrolidone (NMP) and dichloromethane (DCM). Deprotection was achieved using 20% pipiredine in DMF.

Peptides were then cleaved from the resin, with concomitant removal of sidechain protecting groups by treatment with trifluoroacetic acid (TFA; 80%), thioanisol (12%), 1,2-ethanedithol (EDT; 6%), and *m*-cresol (2%). After cleavage, the peptides were precipitated with 2 volumes of cold ether for 10 min, collected by centrifugation, washed two times with cold ether, and left to dry overnight. Purification was carried out by reversed-phase HPLC (Waters 741 Data Module, Waters 484 Tunable Absorbance Detector; Waters 600E System Controller). Samples of crude peptide were chromatographed on a Waters Delta-Pak™ C_{18} column (40 × 100 mm, 15 μm, 100 Å particles) with linear gradient: Milli-Q water/acetonitrile in 0.1% TFA. Peptide mass was confirmed using matrix-assisted laser desorption time-of-flight (MALDI-TOF) mass spectrometry (Kompact Maldi II, Kratos Analytical, Shimadzu, Japan). Lyophilized peptides were stored desiccated at −30°C.

Formation of Heterodimeric Peptide

The heterodimer, PCI-2K-R, was formed by mixing equimolar amounts (~1 mM in Milli-Q water/0.5% acetic acid) of PCI-2K and PCI-R in 500 ml of Milli-Q water (pH 8.2). After mixing for at least 1 day, the pH was readjusted to 2.2 and the solution was filtered through a 0.45 micron filter and desalted using isocratic conditions (50% acetonitrile) on a Waters Delta-Pak™ C_{18} column. The heterodimeric peptide (CPI-2KR) was separated from the monomeric (PCI-2K and PCI-R) and homodimeric species using linear gradient conditions identical to those outlined in the Peptide Synthesis section (above).

The formation of disulfide bonds was indirectly determined by monitoring the absence of SH groups. Ellman's reagent (DTNB; 5,5′-Dithio-*bis*(2-nitrobenzoic acid); 0.1 mM [41]) in potassium dihydrogen phosphate (1.2 mM), disodium hydrogen phosphate buffer (95 mM) forms a mixed disulfide with thiols, liberating the chromophore 5-mercapto-2-nitrobenzoic acid (absorption maximum 410 nm, ϵ ~13, 600 $cm^{-1}M^{-1}$). Peptide solutions (0.25 μM) were mixed with increasing concentrations of Ellman's reagent (0, 0.03, 0.06, 0.075 μM) and read at 412 nm.

Cellulose-Bound Peptide Synthesis

Cellulose-bound overlapping peptides (10-mers) derived from PCI were prepared using an Auto-Spot Robot ASP 222 peptide synthesiser (ABiMED, Langenfeld, Germany; Software DIGEN, Jerini BioTools GmbH, Berlin, Germany) on Whatman 50 (Whatman, Maidstone, United Kingdom) membranes [42]. Anchor groups were obtained by homogeneous derivatisation of the hydroxyl groups with Fmoc-β-alanine. Following deprotection using 20% pipiredine in DMF, Fmoc amino acids (0.5 M), activated using HOBT and *N*, *N*′-diisopropylcarbodiimide (DIPCI), were applied and allowed to react for 20 min. After 10 cycles, the sidechain protecting groups were removed using trifluoroacetic acid (TFA; 80%), thioanisol (12%), 1,2-ethanedithol (EDT; 6%), and *m*-cresol (2%).

Membranes were washed four times with phosphate buffered saline/0.05% Tween20 (pH 7.3; PBS-T) and blocked with PBS-T-1% BSA overnight at 4°C. CPR (10 μg/ml in blocking solution) or PBS-T-1% BSA (control) were allowed to interact with the bound peptides at 4°C overnight. The following day, membranes were incubated with an FITC-conjugated anti-proCPR monoclonal antibody, 10G1 (10G1-FITC; 10 μg/ml), which also recognizes CPR [43], subsequent to being washed four times with PBS-T, twice with PBS-T-1M NaCl, and twice with PBS-T. After 4 hr incubation at room temperature, the membranes were read on a fluorescence laser scanner (FLA3000; Fujifilm, Japan) and analyzed using the Array Gauge software (version 1.0; Fujifilm, Japan).

Purification of proCPR and CPN

ProCPR was purified to homogeneity as previously described [3]. The pure enzyme showed a single band by SDS-polyacrylamide gel electrophoresis (SDS-PAGE) at 60 kDa and was converted by thrombin/thrombomodulin to the activated form resulting in a band at approximately 35 kDa in SDS-PAGE analysis. CPN was purified to homogeneity as previously described [8]. The enzyme gave three bands on SDS-PAGE at 83 kDa, 53 kDa, and 50 kDa, corresponding to the two large identical glycosylated subunits and the two smaller active subunits, respectively.

Hippuryl-L-Arginine Hydrolysis Assay

Carboxypeptidase activity for CPR and CPN samples used for the enzyme kinetics and fibrinolysis assay experiments was determined by use of hippuryl-L-arginine (Peptide Institute Inc., Osaka, Japan) as described previously [44]. Briefly, 30 mM hippuryl-L-arginine in 50 mM HEPES (pH 8.2) was incubated with test samples at 37°C for 45 min, and released hippuric acid was quantitated by HPLC following extraction with ethyl acetate.

Enzyme Kinetics for CPR

The activity of the CPR inhibitors was determined against hippuryl-L-arginine cleavage by purified CPR. The peptides PCI-2K-R, CPI-2KR, PCI (500, 250/125/62.5, 50 μg/ml, respectively) or Tris-HCl buffer (50 mM; pH 7.5) were added to active CPR (40–320 μg/ml) at a 1:7 ratio. After thorough mixing, 20 μl was incubated with various concentrations of hippuryl-L-arginine (1.2–6.0 mM), for 15 min at 37°C [21]. Contrary to the reported procedure (HCl addition, followed by NaOH neutralization), the reaction was stopped with the addition of sodium phosphate buffer (100 μl; 0.25 M), immediately followed by 3% cyanuric chloride in 1,4-dioxane (75 μl). After mixing well, the generation of hippuric acid was determined by measuring the OD at 405 nm on a SpectraMAX 250 Microplate Spectrophotometer (Molecular Device Corporation, Sunnyvale, CA, USA). Hippuric acid (0–2.0 mM) in Tris buffer was used as the standard.

A kinetics analysis of the CPR-catalysed hydrolysis of hippuryl-L-arginine in the absence and presence of inhibitory molecules was performed. The Lineweaver-Burk reciprocal plot, based on rearrangement of the Henri-Michaelis-Menten equation into a linear form, was applied:

$$\frac{1}{v} = \frac{K_m}{V_{max}} \frac{1}{[S]} + \frac{1}{V_{max}}$$

where v (in $mM \cdot s^{-1}$) is the instantaneous or initial velocity, [S] (mM) is the substrate concentration, K_m (mM) is equivalent to the substrate concentration that yields half-maximal velocity, and V_{max} ($mM \cdot s^{-1}$) is the maximum velocity. For competitive inhibition, where the inhibitor competes with the substrate for binding to the enzyme, the following mechanism was assumed:

$$E + S \underset{k-1}{\overset{k_1}{\rightleftharpoons}} ES \xrightarrow{k_2} P$$

$$+$$

$$I \qquad \text{where } K_i = \frac{[E][I]}{[EI]}$$

$$K_i \uparrow\downarrow$$

$$EI$$

In competitive inhibition, the apparent V_{max} is not affected by increasing inhibitor concentrations because once substrate binds, the reaction proceeds normally (i.e., V_{max} depends only on maximum ES complex concentration, which only depends on the total amount of enzyme present). However, the apparent K_m increases (i.e. a higher substrate concentration is required for a given velocity) by a factor of $[1 + ([I]/K_i)]$. Therefore, the dissociation constant for a competitive inhibitor, K_i, can be calculated from:

$$K_{m_{app}} = K_m \left(1 + \frac{[I]}{K_i}\right)$$

where $K_{m_{app}}$ is the apparent K_m for a given inhibitor concentration.

The Dixon plot (1/v versus [I] in the presence of different concentrations of substrate) provides a more diagnostic way of identifying the type of inhibition and determining the K_i:

$$\frac{1}{v} = \frac{K_m}{V_{max} K_i [S]}[I] + \frac{1}{V_{max}}\left(1 + \frac{K_m}{[S]}\right)$$

Since a linear mixed-type inhibitor yields the same type of Dixon plot as a competitive inhibitor, the slopes of the Dixon plots versus 1/[S] can be replotted to distinguish one from the other. For a competitive inhibitor, the slope replot goes through the origin, while that for a mixed-type inhibitor does not.

Enzyme Kinetics for CPN

The effect of CPI-2KR on purified CPN was determined using hippuryl-L-arginine as the substrate. Guanidinoethylmercaptosuccinic acid (GEMSA) was used as a positive control. CPI-2KR (500 μg/ml), GEMSA (100, 500 μg/ml), or Tris-HCl buffer (50 mM; pH 7.5) was added to CPN (10 μg/ml) at a 1:7 ratio. Identical conditions to those used for the CPR kinetics experiments were subsequently applied.

In Vitro Fibrinolysis Assay

Human plasma was obtained by centrifugation of citrated blood at 3000 × g for 15 min at room temperature. In a 96-well microtiter plate, 20 μl of a thrombin/calcium mix (50 μl calcium [$CaCl_2$; 1 M], 20 μl of thrombin [T; 500 U/ml], and 430 μl of Tris buffer [50 mM, pH 7.5]) was added, followed by 10 μl of thrombomodulin (TM; final concentration 8 nM). Subsequently, 10 μl of peptide solution in Tris buffer (16 μg/ml–500 μg/ml), Tris buffer, or PCI (50 μg/ml) was added. After the addition of 50 μl of a t-PA/plasma mix (8 μl of t-PA [130 μg/ml] mixed with 1 ml of prewarmed citrated plasma [37°C for 5 min]), the plate was immediately read at 420 nm every 5 min for 2 hr on a SpectraMAX 250 Microplate Spectrophotometer (Molecular Device Corporation, Sunnyvale, CA, USA). Lysis time was defined as the time required for the absorbance to reach half the difference between the plateau reached after clotting and baseline achieved at clot lysis.

Nuclear Magnetic Resonance Studies

Samples were prepared by dissolving CPI-2KR or CPI-2KR-cyclic in 500 μl of water containing 10% D_2O. The final peptide concentration of the solution was 3 mM. The pH of the sample solution was adjusted to 5.0. NMR experiments were carried out at 5°C on a Bruker DMX-500 spectrometer. Two-dimensional NMR experiments including HOHAHA [45] and ROESY [46] were carried out using the WATERGATE scheme for water suppression [47], while in the case of DQF-COSY [48], a low-power irradiation of the water frequency was used during the relaxation delay. HOHAHA spectra were recorded with mixing time of 60 ms. ROESY spectra were recorded with mixing times of 200 ms, 300 ms, and 400 ms. Processing and analyses of the spectra were done using the Bruker XWINNMR.

Interproton distance constraints were obtained from the ROESY spectra observed with mixing times of 300 ms. Observed ROE data were classified into four distance ranges, 1.8–2.7 Å, 1.8–3.5 Å, 1.8–5.0 Å, and 3.0–6.0 Å, corresponding to strong, medium, weak, and very weak ROE values, respectively. The upper boundary of ROEs involving amide protons was extended to 2.9 Å for strong ROEs and to 3.5 Å for medium ROEs to account for the higher observed intensity of this type of intensity [49]. In addition, a 0.5 Å correction [49] was added to the upper boundary of the distances involving methyl protons. Structure calculations were performed on 41 interproton distance constraints derived from the 2D ROESY spectrum, 7 dihedral angle constraints derived from ^1H 1D-NMR spectrum, and one disulfide bond restraint. All calculations were carried out using dynamic simulated annealing protocols in the program DYNAMO. The structure was analyzed using the program PROCHECK [50].

Molecular Modeling Studies

A conformational search for the global energy minimum of the molecules (PCI-2K-R, CPI-2KR, and CPI-2KR-cyclic) was performed in vacuo using a molecular dynamics (MD) simulated annealing strategy. The consistent-valence forcefield (CVFF) was used for the potential energy calculations, which included all bond, torsion, out-of-plane, and nonbond van der Waals and electrostatic terms. A cutoff distance of 13 Å was used for the calculation of the nonbond interaction energy (van der Waals and electrostatic terms) and a dielectric constant of 1 was used for the calculation of the electrostatic energy. Initially, to relax the peptides from strain, a steepest descent minimization was applied for 5,000 iterations, until a maximum derivative of less than 1.00 kcal/Å was achieved. This was followed by conjugate gradient minimization for 10,000 iterations, until a maximum derivative of 0.01 kcal/Å was achieved. The system was subsequently

equilibrated at 200 K for 10 ps and then rapidly heated to 900 K by increasing the temperature by 100 K every 1 ps. The configuration space was sampled at 900 K for 10 ps. After the high temperature dynamics, the system was cooled slowly by decreasing the temperature by 25 K every 1 ps, until the temperature reached 200 K. At this stage the system was reequilibrated for a further 10 ps and the configuration space was sampled once again for 30 ps. The lowest energy conformation of each peptide from the MD simulation was selected for analysis. The C_α-C_α distances between the basic residues of each peptide were measured using InsightII (MSI, San Diego).

Circular Dichroism Spectropolarimetry

Circular dichroism spectra were measured over the range 190–250 nm, using a Jasco-715 spectropolarimeter (Jasco, Tokyo, Japan) coupled to an Eyela Cooling Thermo Pump CTP-200 (Tokyo Rikakikai Co. Ltd, Tokyo, Japan). Spectra were obtained in Tris-HCl (50 mM, pH 7.5) at 4°C using a cell with a path length of 0.1 cm. CPR (40 μg/ml) and CPI-2KR (160 μg/ml) concentrations were similar to those used for the kinetics studies. Data points were recorded at a scan speed of 50 nm/min, bandwidth of 1.0 nm, 8 s response, and 0.1 nm resolution. Four repeat scans were used to obtain the final averaged spectra. Following baseline correction, the observed ellipticity, θ, was converted to mean residue ellipticity [θ] (deg cm^2 $dmole^{-1}$), using the relationship:

$$[\Theta] = \frac{\Theta}{10 \cdot lcN}$$

where *l* is the path length in centimeters, *c* is the molar concentration, and *N* is the number of residues in the protein/peptide. The percentage of α helix, β sheet, β turn, and random structure was estimated using the least squares method [51] and reference CD spectra [52] using the Protein Secondary Structure Estimation software V1.10.00 (Jasco, Tokyo, Japan).

Acknowledgments

The technical advice of Dr. Mitsukoshi Kunimatsu is much appreciated for the spot peptide membrane synthesis. This work was supported by a research grant from the Organization for Pharmaceutical Safety and Research of Japan.

Received: June 21, 2002
Revised: September 5, 2002
Accepted: September 11, 2002

References

1. Vendrell, J., Querol, E., and Aviles, F.X. (2000). Metallocarboxypeptidases and their protein inhibitors. Structure, function and biomedical properties. Biochim. Biophys. Acta *1477*, 284–298.
2. Campbell, W., and Okada, H. (1989). An arginine specific carboxypeptidase generated in blood during coagulation or inflammation which is unrelated to carboxypeptidase N or its subunits. Biochem. Biophys. Res. Commun. *162*, 933–939.
3. Eaton, D.L., Malloy, B.E., Tsai, S.P., Henzel, W., and Drayna, D. (1991). Isolation, molecular cloning, and partial characterization of a novel carboxypeptidase B from human plasma. J. Biol. Chem. *266*, 21833–21838.
4. Hendriks, D., Scharpe, S., van Sande, M., and Lommaert, M.P. (1989). Characterization of a carboxypeptidase in human serum distinct from carboxypeptidase N. J. Clin. Chem. Clin. Biochem. *27*, 277–285.
5. Bajzar, L., Manuel, R., and Nesheim, M.E. (1995). Purification and characterization of TAFI, a thrombin-activable fibrinolysis inhibitor. J. Biol. Chem. *270*, 14477–14484.
6. Reynolds, D.S., Gurley, D.S., Stevens, R.L., Sugarbaker, D.J., Austen, K.F., and Serafin, W.E. (1989). Cloning of cDNAs that encode human mast cell carboxypeptidase A, and comparison of the protein with mouse mast cell carboxypeptidase A and rat pancreatic carboxypeptidases. Proc. Natl. Acad. Sci. USA *86*, 9480–9484.
7. Campbell, W., Okada, N., and Okada, H. (2001). Carboxypeptidase R is an inactivator of complement-derived inflammatory peptides and an inhibitor of fibrinolysis. Immunol. Rev. *180*, 162–167.
8. Plummer, T.H., Jr., and Hurwitz, M.Y. (1978). Human plasma carboxypeptidase N. Isolation and characterization. J. Biol. Chem. *253*, 3907–3912.
9. Plummer, T.H., Jr., and Ryan, T.J. (1981). A potent mercapto bi-product analogue inhibitor for human carboxypeptidase N. Biochem. Biophys. Res. Commun. *98*, 448–454.
10. Tan, F., Jackman, H., Skidgel, R.A., Zsigmond, E.K., and Erdos, E.G. (1989). Protamine inhibits plasma carboxypeptidase N, the inactivator of anaphylatoxins and kinins. Anesthesiology *70*, 267–275.
11. Skidgel, R.A., Deddish, P.A., and Davis, R.M. (1988). Isolation and characterization of a basic carboxypeptidase from human seminal plasma. Arch. Biochem. Biophys. *267*, 660–667.
12. Shinohara, T., Sakurada, C., Suzuki, T., Takeuchi, O., Campbell, W., Ikeda, S., Okada, N., and Okada, H. (1994). Pro-carboxypeptidase R cleaves bradykinin following activation. Int. Arch. Allergy Immunol. *103*, 400–404.
13. Campbell, W., Lazoura, E., Okada, N., and Okada, H. (2002). Inactivation of C3a and C5a octapeptides by carboxypeptidase R and carboxypeptidase N. Microbiol. Immunol. *46*, 131–134.
14. Redlitz, A., Tan, A.K., Eaton, D.L., and Plow, E.F. (1995). Plasma carboxypeptidases as regulators of the plasminogen system. J. Clin. Invest. *96*, 2534–2538.
15. Christensen, U. (1985). C-terminal lysine residues of fibrinogen fragments essential for binding to plasminogen. FEBS Lett. *182*, 43–46.
16. Fleury, V., and Angles-Cano, E. (1991). Characterization of the binding of plasminogen to fibrin surfaces: the role of carboxy-terminal lysines. Biochemistry *30*, 7630–7638.
17. Vali, Z., and Patthy, L. (1984). The fibrin-binding site of human plasminogen. Arginines 32 and 34 are essential for fibrin affinity of the kringle 1 domain. J. Biol. Chem. *259*, 13690–13694.
18. Nicole, O., Docagne, F., Ali, C., Margaill, I., Carmeliet, P., MacKenzie, E.T., Vivien, D., and Buisson, A. (2001). The proteolytic activity of tissue-plasminogen activator enhances NMDA receptor-mediated signaling. Nat. Med. *7*, 59–64.
19. Nagashima, M., Werner, M., Wang, M., Zhao, L., Light, D.R., Pagila, R., Morser, J., and Verhallen, P. (2000). An inhibitor of activated thrombin-activatable fibrinolysis inhibitor potentiates tissue-type plasminogen activator-induced thrombolysis in a rabbit jugular vein thrombolysis model. Thromb. Res. *98*, 333–342.
20. Ryan, C.A., Hass, G.M., and Kuhn, R.W. (1974). Purification and properties of a carboxypeptidase inhibitor from potatoes. J. Biol. Chem. *249*, 5495–5499.
21. Mosnier, L.O., dem Borne, P.A., Meijers, J.C., and Bouma, B.N. (1998). Plasma TAFI levels influence the clot lysis time in healthy individuals in the presence of an intact intrinsic pathway of coagulation. Thromb. Haemost. *80*, 829–835.
22. Bajzar, L., Morser, J., and Nesheim, M. (1996). TAFI, or plasma procarboxypeptidase B, couples the coagulation and fibrinolytic cascades through the thrombin-thrombomodulin complex. J. Biol. Chem. *271*, 16603–16608.
23. Boffa, M.B., Wang, W., Bajzar, L., and Nesheim, M.E. (1998). Plasma and recombinant thrombin-activable fibrinolysis inhibitor (TAFI) and activated TAFI compared with respect to glycosylation, thrombin/thrombomodulin-dependent activation, thermal stability, and enzymatic properties. J. Biol. Chem. *273*, 2127–2135.
24. Esmon, C.T. (2000). The endothelial cell protein C receptor. Thromb. Haemost. *83*, 639–643.
25. Mosnier, L.O., Meijers, J.C., and Bouma, B.N. (2001). Regulation of fibrinolysis in plasma by TAFI and protein C is dependent on the concentration of thrombomodulin. Thromb. Haemost. *85*, 5–11.
26. Kato, T., Akatsu, H., Sato, T., Matsuo, S., Yamamoto, T., Campbell, W., Hotta, N., Okada, N., and Okada, H. (2000). Molecular cloning and partial characterization of rat procarboxypeptidase R and carboxypeptidase N. Microbiol. Immunol. *44*, 719–728.
27. Sato, T., Miwa, T., Akatsu, H., Matsukawa, N., Obata, K., Okada,

N., Campbell, W., and Okada, H. (2000). Pro-carboxypeptidase R is an acute phase protein in the mouse, whereas carboxypeptidase N is not. J. Immunol. *165*, 1053–1058.
28. van Tilburg, N.H., Rosendaal, F.R., and Bertina, R.M. (2000). Thrombin activatable fibrinolysis inhibitor and the risk for deep vein thrombosis. Blood *95*, 2855–2859.
29. Martineau, B., McBride, K.E., and Houck, C.M. (1991). Regulation of metallocarboxypeptidase inhibitor gene expression in tomato. Mol. Gen. Genet. *228*, 281–286.
30. Homandberg, G.A., Litwiller, R.D., and Peanasky, R.J. (1989). Carboxypeptidase inhibitors from Ascaris suum: the primary structure. Arch. Biochem. Biophys. *270*, 153–161.
31. Reverter, D., Vendrell, J., Canals, F., Horstmann, J., Aviles, F.X., Fritz, H., and Sommerhoff, C.P. (1998). A carboxypeptidase inhibitor from the medical leech Hirudo medicinalis. Isolation, sequence analysis, cDNA cloning, recombinant expression, and characterization. J. Biol. Chem. *273*, 32927–32933.
32. Normant, E., Martres, M.P., Schwartz, J.C., and Gros, C. (1995). Purification, cDNA cloning, functional expression, and characterization of a 26-kDa endogenous mammalian carboxypeptidase inhibitor. Proc. Natl. Acad. Sci. USA *92*, 12225–12229.
33. McKay, T.J., and Plummer, T.H., Jr. (1978). By-product analogues for bovine carboxypeptidase B. Biochemistry *17*, 401–405.
34. Schatteman, K.A., Goossens, F.J., Scharpe, S.S., Neels, H.M., and Hendriks, D.F. (1999). Assay of procarboxypeptidase U, a novel determinant of the fibrinolytic cascade, in human plasma. Clin. Chem. *45*, 807–813.
35. Klement, P., Liao, P., and Bajzar, L. (1999). A novel approach to arterial thrombolysis. Blood *94*, 2735–2743.
36. Bouma, B.N., Marx, P.F., Mosnier, L.O., and Meijers, J.C. (2001). Thrombin-activatable fibrinolysis inhibitor (TAFI, plasma procarboxypeptidase B, procarboxypeptidase R, procarboxypeptidase U). Thromb. Res. *101*, 329–354.
37. Craik, D.J., Daly, N.L., and Waine, C. (2001). The cystine knot motif in toxins and implications for drug design. Toxicon *39*, 43–60.
38. Rees, D.C., and Lipscomb, W.N. (1980). Structure of the potato inhibitor complex of carboxypeptidase A at 2.5-Å resolution. Proc. Natl. Acad. Sci. USA *77*, 4633–4637.
39. Rees, D.C., and Lipscomb, W.N. (1980). Structure of potato inhibitor complex of carboxypeptidase A at 5.5-Å resolution. Proc. Natl. Acad. Sci. USA *77*, 277–280.
40. Hendriks, D., Wang, W., Scharpe, S., Lommaert, M.P., and van Sande, M. (1990). Purification and characterization of a new arginine carboxypeptidase in human serum. Biochim. Biophys. Acta *1034*, 86–92.
41. Ellman, G.L. (1959). Tissue sulfhydryl groups. Arch. Biochem. Biophys. *82*, 70–77.
42. Frank, R. (1992). SPOT synthesis: an easy technique for the positionally addressable, parallel chemical synthesis on a membrane support. Tetrahedron *48*, 9217–9232.
43. Guo, X., Morioka, A., Kaneko, Y., Okada, N., Obata, K., Nomura, T., Campbell, W., and Okada, H. (1999). Arginine carboxypeptidase (CPR) in human plasma determined with sandwich ELISA. Microbiol. Immunol. *43*, 691–698.
44. Watanabe, M., Ishikawa, Y., Campbell, W., and Okada, H. (1998). Measurement of arginine carboxypeptidase-generating activity of adult plasma. Microbiol. Immunol. *42*, 393–397.
45. Bax, A., and Davis, D.G. (1985). MLEV-17-based two-dimentional homonuclear magnetization transfer spectroscopy. J. Magn. Reson. *65*, 355–360.
46. Bothner-By, A.A., Stephens, R.L., Lee, J.M., Warren, C.D., and Jeanloz, R.W. (1984). Structure determination of a tetrasaccharide: Transient nuclear Overhauser effects in the rotating frame. J. Am. Chem. Soc. *106*, 811–813.
47. Piotto, M., Saudek, V., and Sklenar, V. (1992). Gradient-tailored excitation for single quantum spectroscopy of aqueous solutions. J. Biomol. NMR *2*, 661–665.
48. Rance, M., Sorencen, O.W., Bodenhausen, G., Wagner, G., Ernst, R.R., and Wüthrich, K. (1993). Improved spectral resolution in COSY ^{1}H NMR spectra of proteins via double quantum filtering. Biochem. Biophys. Res. Commun. *117*, 479–485.
49. Qin, J., Clore, G.M., Kennedy, W.P., Kuszeuski, J., and Gronenborn, A.M. (1996). The solution structure of human thioredoxin complexed with its target from Ref-1 reveals peptide chain reversal. Structure *4*, 613–620.
50. Laskowski, R.A., MacArthur, M.W., Moss, D.S., and Thornton, J.M. (1993). PROCHECK: a program to check the stereochemical quality of protein structures. J. Appl. Crystallogr. *26*, 283–291.
51. Provencher, S.W., and Glöckner, J. (1981). Estimation of globular protein secondary structure from circular dichroism. Biochemistry *20*, 33–37.
52. Yang, J.T., Wu, C.-S., and Martinez, H.M. (1986). Calculation of protein conformation from circular dichroism. Methods Enzymol. *130*, 208–269.